Proc. Natl. Acad. Sci. USA
Vol. 89, pp. 10494–10498, November 1992
Physiology

Molecular characterization and nephron distribution of a family of transcripts encoding the pore-forming subunit of Ca^{2+} channels in the kidney

(epithelial ion channels/cDNA cloning/polymerase chain reaction)

ALAN S. L. YU, STEVEN C. HEBERT, BARRY M. BRENNER, AND JONATHAN LYTTON*

Laboratory of Molecular Physiology and Biophysics, Renal Division, Department of Medicine, Brigham & Women's Hospital and Harvard Medical School, Boston, MA 02115

Communicated by Robert W. Berliner, July 15, 1992

ABSTRACT **Active, transepithelial, Ca^{2+} reabsorption in kidney occurs primarily in the distal convoluted tubule. Recent evidence suggests that entry of Ca^{2+} at the apical membrane through channels bearing resemblance to those of the voltage-dependent L type may be the rate-determining step in Ca^{2+} reabsorption. To determine the molecular identity of the pore-forming subunit of voltage-dependent Ca^{2+} channel(s) in the kidney, a homology-based PCR cloning strategy was employed. Nondegenerate primers, based on conserved regions of the published cDNA sequences of voltage-dependent Ca^{2+} channel α_1 subunits, were used to amplify cDNA from rat kidney, and the products were subcloned and sequenced. A family of molecular species was identified, representing alternatively spliced transcripts of four known genes encoding these channel subunits. Northern blot analysis indicated that the expression of each of the genes exhibits a distinct spatial distribution within the kidney. One gene, CaCh4, is expressed primarily in the cortex, and by microdissected-tubule PCR was found predominantly in the distal convoluted tubule, consistent with a role in transepithelial Ca^{2+} reabsorption at this site.**

Epithelial cells are unique in their ability to mediate vectorial transport of ions such as Ca^{2+} between apical and basolateral surfaces, but the underlying molecular mechanisms are poorly understood. The distal nephron of the kidney serves as a paradigm for Ca^{2+} absorptive epithelia. Although Ca^{2+} filtered at the glomerulus is reabsorbed along the whole length of the nephron, active, and therefore transcellular, transport has been demonstrated primarily in distal convoluted tubule (1) and, to a lesser extent, in cortical thick ascending limb (2), the same sites at which parathyroid hormone (PTH) has its hypocalciuric effect. Recent evidence implicates Ca^{2+} entry at the apical membrane as the rate-determining step in active Ca^{2+} reabsorption and suggests that it is mediated by a PTH-activated pathway that is sensitive to 1,4-dihydropyridine (DHP) compounds (3). This indicates involvement of Ca^{2+} channels resembling those of the voltage-dependent L type, a contention that is supported by patch clamp analysis. Although various cation channels have been found in the apical membranes of tubule epithelial cells, the only Ca^{2+}-selective ones observed have been of the voltage-dependent type (4–7).

In contrast to epithelial cells, voltage-dependent Ca^{2+} channels have been well characterized in excitable cells (8), and at least four types (L, N, T, and P) can be distinguished on the basis of electrophysiological and pharmacological properties. L-type Ca^{2+} channels in skeletal muscle, where they are most abundant, are composed of five different subunits, of which the largest, the 170-kDa α_1 subunit, forms the ion pore. cDNA cloning has demonstrated at least five distinct, but homologous, genes that encode the α_1 subunit. According to the order in which they were described, we refer to them as CaCh1 (9), CaCh2 (10), CaCh3 (11), CaCh4 (12), and CaCh5 (13), following the nomenclature introduced by Perez-Reyes *et al.* (14). Their deduced general primary structures are similar, and each has four internally repeated domains (I–IV), each containing six potential membrane-spanning segments (S1–S6). Further heterogeneity is afforded by alternative splicing of transcripts, which occurs at multiple different sites. Of note, in three of these genes a splice site involving the IV–S3 region is conserved (14).

Functional expression of CaCh1, -2, and -3 (10, 15, 16) yields Ca^{2+} currents with properties similar to those of native L-type channels, including DHP sensitivity. CaCh4 appears to encode a voltage-dependent Ca^{2+} channel that is insensitive to either DHP or ω-conotoxin GVIA (an N-type channel antagonist) but is inhibited by the toxin of the funnel web spider, *Agelenopsis aperta* (12), a characteristic of P-type channels (17), while CaCh5 is a specific receptor for ω-conotoxin GVIA (13). Thus, members of this gene family encode pore-forming units of Ca^{2+} channels with potentially disparate properties that cross the boundaries of conventional classification. Furthermore, each gene exhibits a different pattern of tissue-specific expression, yet how this relates to the distinct functional properties of each channel that it encodes remains to be elucidated.

To determine the molecular identity of the Ca^{2+} channel α_1 subunit(s) expressed in kidney, we used a homology-based polymerase chain reaction (PCR) cloning strategy. We have characterized a family of renal Ca^{2+} channel α_1-subunit isoforms, representing transcripts of all four genes, as well as alternatively spliced variants.† One gene, CaCh4, is predominantly expressed in distal convoluted tubule (DCT), consistent with a role in transepithelial Ca^{2+} transport.

METHODS

Standard protocols were used (18), except where noted.

Design of PCR Primers. See Fig. 1*A*. Regions, flanking the IV-S6 transmembrane domain, with nucleotide identity between the published rabbit CaCh1 (9) and CaCh2 (10) cDNA sequences were initially selected for the design of nondegenerate oligonucleotide primers, Cc1 (5′-AACAACAACTTC-CAGACCTTC-3′) (sense) and Cc2 (5′-GGGTCATACTCT-GCCCAGAT-3′) (antisense). Cc1 and -2 are predicted to

The publication costs of this article were defrayed in part by page charge payment. This article must therefore be hereby marked "*advertisement*" in accordance with 18 U.S.C. §1734 solely to indicate this fact.

Abbreviations: DHP, dihydropyridine; DCT, distal convoluted tubule.

*To whom reprint requests should be addressed at: Renal Division, Brigham & Women's Hospital, 75 Francis St., Boston, MA 02115.

†The sequences of clones RKC2, RKC6, and RKC8 reported in this paper have been deposited in the GenBank data base (accession nos. M99220, M99221, and M99222, respectively).

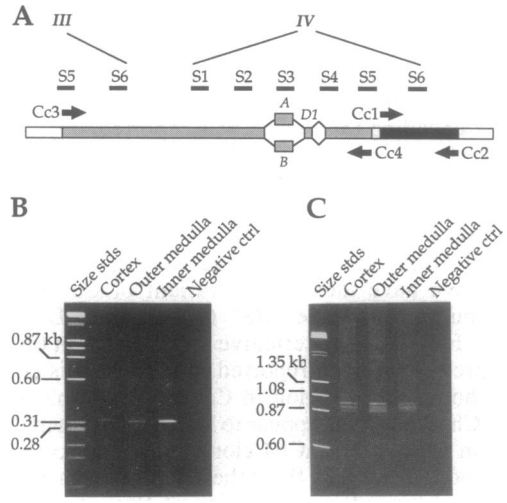

FIG. 1. Detection of renal Ca^{2+} channel α_1-subunit gene expression by PCR. (*A*) Location of primer sequences relative to transmembrane domains (S1–S6) of the third and fourth internal repeat and to the IV-S3 splice site [diagram based on the structure of CaCh2 (19)]. (*B* and *C*) Cc1/2 (*B*) and Cc3/4 (*C*) primer pairs were used to amplify first-strand cDNA from the indicated regions of rat kidney or in the absence of template (Negative ctrl). Products and molecular size standards (*Hin*dIII-digested λ DNA and *Hae* III-digested φX174 DNA) were electrophoresed in 5% polyacrylamide gels and stained with ethidium bromide.

amplify a 326- to 332-base-pair (bp) fragment. A further pair of primers was subsequently designed, using regions of nucleotide sequence highly conserved between rat CaCh2 (20), CaCh3 (11), and CaCh4 (21) and rabbit CaCh1 (for which the rat sequence is unknown). Cc3 (5′-GTCCAGCTCT-TCAAGGGGAA-3′) (sense) and Cc4 (5′-CCAAACATCTG-CATCCCAAT-3′) (antisense), corresponding to regions within III-S5 and IV-S5, respectively, are predicted to amplify a fragment approximately 1 kilobase (kb) in size, including the commonly spliced IV-S3 region. Primers specific for rat β-actin, Ac1 (5′-TCCTAGCACCATGAAGATC-3′) (sense) and Ac2 (5′-AAACGCAGCTCAGTAACAG-3′) (antisense), corresponding to nucleotides 2845–2863 and 3140–3158, respectively (22), were chosen to span a single intron, thus allowing amplification products from cDNA and genomic DNA to be distinguished.

PCR. All PCR mixes contained 50 mM KCl, 10 mM Tris·HCl at pH 8.3, 1.0–2.5 mM $MgCl_2$ (optimized for each primer pair), gelatin at 0.01 mg/ml, each deoxynucleoside triphosphate at 200 μM, each primer at 250 nM, and 0.5 unit of *Taq* DNA polymerase (Pharmacia) in a total volume of 20 μl. For PCR of kidney regions macroscopically dissected from adult male CD rats (Charles River Breeding Laboratories), 1 μg of total RNA, isolated by the guanidinium isothiocyanate/CsCl method, was reverse transcribed for 1 hr at 37°C with 200 units of Superscript Moloney murine leukemia virus reverse transcriptase (BRL), in the buffer supplied by the manufacturer, using an oligo(dT) primer, in a total volume of 20 μl, and the reaction was terminated by heating to 95°C for 5 min. Four microliters of this first-strand cDNA was added to each PCR mixture. For PCR of microdissected tubule segments (see below), 2 μl of first-strand cDNA was added. Amplification was performed at "high stringency," using a programmable thermal cycler with an in-sample temperature probe (PTC100, MJ Research, Watertown, MA) as follows: 92°C, 2 min (initial melt); 30 cycles of 92°C, 10 s/55°C, 1 min/72°C, 2 min; then 72°C, 5 min (final extension). Reamplification of tubule samples was performed by diluting 2 μl of first-round product into a fresh 20-μl reaction mixture and amplifying with the same protocol for a further 30 cycles. "Low-stringency" PCR to detect novel isoforms was performed as follows: 92°C, 2 min; 5 cycles of 92°C, 10 s/37°C, 1 min/72°C, 2 min; 25 cycles of 92°C, 10 s/55°C, 1 min/72°C, 2 min; then 72°C, 5 min.

Cloning and Sequencing of PCR Products. Amplified products visible as ethidium bromide-stained bands after gel electrophoresis were excised, purified by binding to Geneclean (Bio 101, La Jolla, CA), made blunt-ended by treatment with the Klenow fragment of DNA polymerase I, and then ligated into the *Sma* I site of pBluescript II SK (-) (Stratagene) for electroporation into *Escherichia coli* DH10B cells (BRL). Colonies were screened by PCR, using the primer sequences incorporated at their termini followed by digestion with the frequently cutting restriction enzymes *Alu* I, *Hae* III, and *Hinf*I, and grouped according to the pattern of fragments. Plasmid DNA was prepared from multiple representative colonies from each group (to detect PCR incorporation errors) and sequenced by the dideoxynucleotide chain-termination method. For inserts longer than 0.5 kb, sequence-specific oligonucleotides were used to obtain overlapping sequences.

Individual Nephron Segment Microdissection. Our protocol was modified from Moriyama *et al.* (23). The left kidney of a 100- to 150-g male CD rat was perfused with 3 ml of bicarbonate-free Dulbecco's modified Eagle's medium (DMEM) (GIBCO) containing type I collagenase at 0.5 mg/ml, protease XXV at 0.5 mg/ml, and 0.0005% antifoam B (all from Sigma). Superficial cortical and horizontal slices were cut and incubated in this solution at 37°C, bubbled with 100% O_2 for 10–30 min, then washed and placed on ice in bicarbonate-free DMEM containing 0.1% bovine serum albumin (Sigma), 0.001% antifoam B, and 10 μM vanadyl ribonucleoside complex (VRC) (BRL). Nephron segments were microdissected in this solution, captured on polylysine-coated glass microbeads (0.5-mm diameter, Thomas), and transferred to a 0.5 ml Eppendorf tube. Particular care was taken to identify DCTs on the basis of continuity with a length of cortical thick ascending limb abutting a glomerulus. One to three beads, each with an adherent tubule 0.25–0.5 mm long, were pooled into a single tube. Glomeruli, four to six per tube, were transferred by direct pipetting. Bead-tubules and glomeruli were immediately rinsed four times with 10 μl of phosphate-buffered saline containing placental RNase inhibitor (Pharmacia) at 1 unit/μl, solubilized with 10 μl of 2% Triton X-100 containing RNase inhibitor at 2 units/μl, and frozen on dry ice until all nephron segments were ready. Samples were reverse transcribed *in situ* by adding to each tube a mix containing oligo(dT) primer and 200 units of Superscript Moloney murine leukemia virus reverse transcriptase (BRL) to make up a total volume of 20 μl, incubated 1 hr at 37°C, and 5 min at 95°C, and stored frozen at −20°C.

Detection of the expression of the housekeeping gene β-actin by PCR was used as a control for the integrity of the tubule RNA. In 65% of samples a β-actin product could be detected by ethidium bromide staining, and only those samples were included in our analysis. Along with each series of tubules, a mock sample containing three microbeads taken from the wash dish, but with no tubules attached, was processed in parallel. In addition, reverse transcriptase was omitted from one sample from each set of tubules taken from a particular nephron segment. All of these controls were negative.

Northern and Southern Blot Analysis. RNA was transferred by capillary diffusion from denaturing agarose gels, and DNA was transferred by electrophoresis from polyacrylamide gels to Duralon nylon membrane (Stratagene) and fixed by UV crosslinking. Riboprobes, synthesized by *in vitro* transcription of inserts in the following pBluescript II SK (-) clones, using T3 or T7 RNA polymerase in the presence of digoxigenin-labeled UTP (Boehringer Mannheim), were hybridized

to blots, washed, and processed for chemiluminescence detection using Lumi-Phos 530 (Boehringer Mannheim), all according to the manufacturer's instructions. The CaCh1 probe was synthesized from our clone RKC2 (see *Results*); the CaCh2 probe, from a 332-bp clone of a Cc1/2 amplified product from rat vascular smooth muscle (K.-D. Wu, A.S.L.Y., and J.L., unpublished data) that is 100% identical to the nucleotide sequence of rat CaCh2 (20); CaCh3, from RKC5; and CaCh4, from RKC1.

RESULTS AND DISCUSSION

Identification of Transcripts Encoding Renal Ca^{2+} Channel Isoforms by PCR. Rat kidney total RNA was reverse transcribed and amplified by PCR using primers Cc1 and Cc2. As shown in Fig. 1*B*, a specific product migrating at approximately the predicted size of 320–330 bp can be detected in all regions of the kidney. These bands were excised and subcloned, and 11 colonies were screened by restriction digestion of PCR-amplified inserts. Two different species were identified and several clones of each were sequenced. RKC1 is 317 bp in length and shares 100% nucleotide sequence identity to the corresponding region of rat CaCh4. RKC2 is 326 bp in length and shares 92% nucleotide and 98% amino acid identity (over 285 bp) to the corresponding region of rabbit CaCh1 (Fig. 2*A*), indicating that it corresponds to the rat CaCh1 gene product. PCR using a second pair of primers, Cc3 and Cc4, designed with sequence information available for all four isoforms, yielded multiple products varying in size from 0.9 to 1.1 kb (Fig. 1*C*). Clones corresponding to CaCh2 and CaCh3 were isolated, in addition to CaCh4, from a total of 35 colonies that were screened (Fig. 2*B*). Thus, the expression of four of the known voltage-dependent Ca^{2+} channel α_1-subunit genes can be detected in kidney by PCR.

Sequencing of Clones Reveals Alternatively Spliced Variants. Screening of multiple clones of products amplified by Cc3 and Cc4 revealed that CaCh2, -3, and -4 in kidney are all alternatively spliced at the IV-S3 site (Fig. 2*B*). Clones corresponding to CaCh2c (RKC3 in Fig. 2*B*), CaCh2d (RKC4), and CaCh3b (RKC5) were found in kidney (for nomenclature, see ref. 14). Recently, the genomic structure of CaCh2 encoding this region was reported (19). An 84-bp region was found to be encoded by one of two exons (S3A or S3B) that are spliced in a mutually exclusive fashion. Immediately downstream of this is a 33-bp region (exon D1) that can be present or absent (Fig. 1*A*). The known splicing pattern of CaCh3 suggests that its gene is likely to be arranged similarly. We have identified a variant of CaCh3 (RKC6) which is missing both the "S3" (84-bp) and "D1" (45-bp) segments. For CaCh4, alternative splicing within this region had not previously been reported, but when it is compared with the homologous region in CaCh2 or CaCh3, the published CaCh4 sequences appear to lack a D1 segment (12, 21). In addition to several CaCh4 clones identical to those previously reported (RKC7), five other clones were isolated that contained a 6-bp in-frame insertion at this site, coding for asparagine and proline (RKC8). These putative novel CaCh3 and CaCh4 splice variants were detected in two samples of kidney RNA independently isolated from separate rats. Together with the observation that the putative splice sites coincide with the known boundaries of previously described alternatively spliced segments, these findings suggest that these species represent genuine transcript variants and not simply PCR artifacts.

"Low-Stringency" PCR Reveals No Further Isoforms in Kidney. To detect any other homologous genes that might be expressed, kidney cortex cDNA was amplified by using a "low-stringency" PCR protocol with a reduced annealing temperature for the first five cycles, and first-round products were reamplified. In addition to previously noted bands of 330 bp and 0.9–1.1 kb in size with Cc1/2 and Cc3/4 primers, respectively, multiple other bands were observed (Fig. 3*A*). Compared with products amplified at "high stringency," more bands were observed by ethidium bromide staining, but

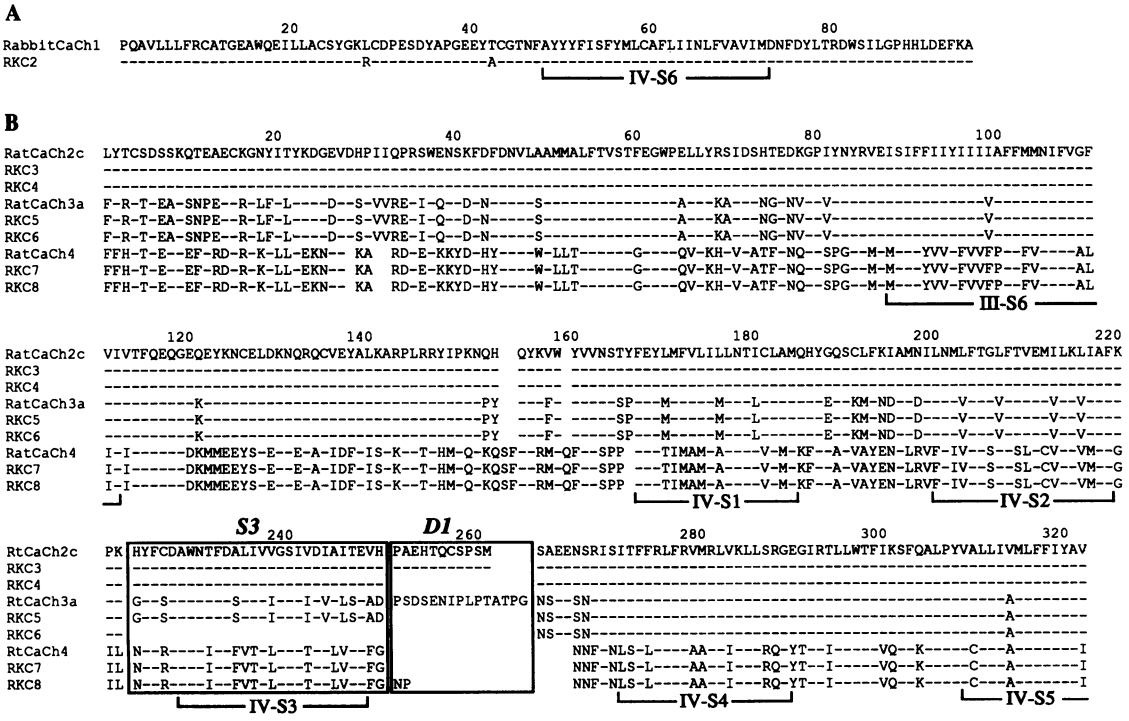

FIG. 2. Comparison of deduced amino acid sequences of renal PCR clones (RKC2–RKC8) of Cc1/2 (*A*) and Cc3/4 (*B*) amplification products to published sequences of rabbit CaCh1 (9) and rat CaCh2c (ref. 20, in which it is called rbC-II), CaCh3a (11), and CaCh4 (21). Dashes indicate identity with residues on the top line and gaps are denoted by spaces. Potential membrane-spanning segments are shown below the corresponding sequences. Boxes delineate the known exon boundaries of the IV-S3 region of CaCh2 (19) and of the homologous regions within the other sequences.

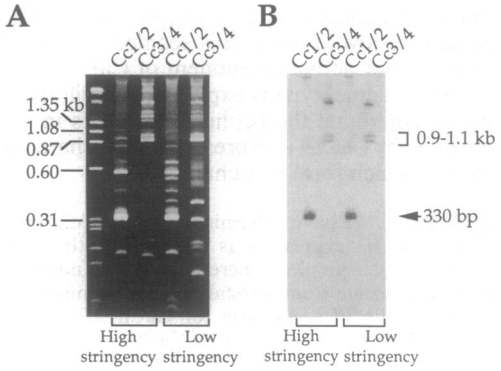

FIG. 3. "Low-stringency" PCR detects no novel isoforms. Kidney cortex RNA was amplified with the indicated primer pairs by using high- or low-stringency cycling protocols, and first-round products were reamplified through a further 30 cycles at high stringency. Second-round products were electrophoresed in a 5% polyacrylamide gel and visualized by ethidium bromide staining (*A*), then transferred to nylon and hybridized to a mixture of CaCh1–4 riboprobes (*B*). The sizes of molecular weight markers (far left lane), and of bands which were cut out for restriction analysis (on the right), are indicated.

blots probed at reduced stringency with a mixture of riboprobes specific for all four isoforms revealed hybridization to apparently identical bands (Fig. 3*B*).

To determine whether any novel isoforms, amplified at low but not at high stringency, comigrated with the 330-bp and 0.9- to 1.1-kb bands, these regions were excised after gel electrophoresis and digested with frequently cutting restriction enzymes. A complicated pattern of fragments was found, reflecting the presence of multiple molecular species, but this pattern was identical in low- and high-stringency-amplified products. Higher molecular weight bands also detected by blot hybridization (Fig. 3*B*) could be reproduced when DNA prepared from one or more clones, each representing a single isoform, was amplified, thus indicating that these were most likely due to the aberrant migration of authentic amplification products.

Northern Blot Analysis of Regional Distribution Within Kidney. Northern blots of RNA from kidney regions and other rat tissues were hybridized to riboprobes specific for each Ca^{2+} channel α_1-subunit gene (Fig. 4). CaCh1 hybridized strongly to a 6.5-kb transcript in skeletal muscle, as previously described (9), and to a 4.5- to 5-kb transcript confined to inner medulla. Interestingly, an alternatively spliced variant of CaCh1 was recently described in neonatal skeletal muscle that contains only two of the usual four internally repeated domains due to an internal deletion, resulting in a 4.4-kb transcript (24), similar in size to the transcript that we observed in kidney. Such a deletion would result in loss of the primer recognition site for Cc3, thus providing a potential explanation for the absence of an amplified CaCh1 product with that primer. CaCh2 hybridized to transcripts of 8.5 and 12 kb in heart, brain, and all regions of the kidney, but particularly the inner medulla. CaCh3 hybridized to a transcript of 9.5 kb in brain and to bands of 9.5 and 12.5 kb in kidney, with preferential localization to the outer medulla. CaCh4 hybridized to a band of 9 kb in brain. In kidney, a similarly sized transcript was found almost exclusively in the cortex. A signal at 6.5 kb found on hybridization of CaCh2, -3, and -4 probes to skeletal muscle was assumed to be due to cross-hybridization to the extremely abundant CaCh1 message in this tissue.

These Northern blots confirm our PCR finding of renal expression of four Ca^{2+} channel α_1-subunit genes and demonstrate that each exhibits a distinct spatial distribution within the kidney. Of note, however, only CaCh4 preferentially localizes to cortex, the region in which active Ca^{2+} reabsorption occurs. Hybridization and washing of identical blots at reduced stringency did not alter the ratio of signal intensities of the observed bands, nor were any novel bands revealed (data not shown), suggesting that no other structurally related genes in addition to these four are expressed in kidney.

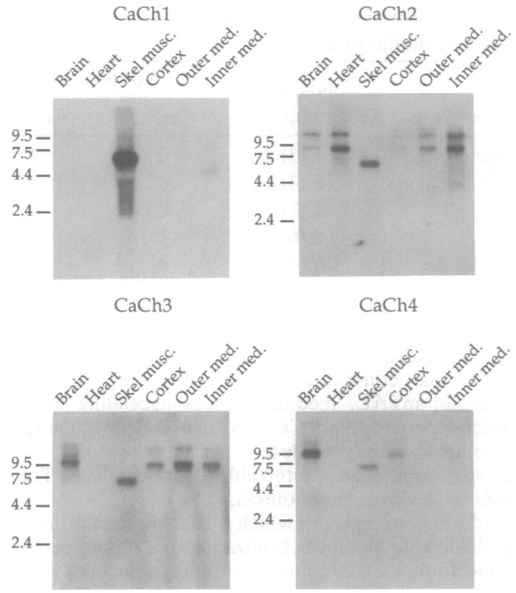

FIG. 4. Northern blots of rat tissues hybridized at high stringency to Ca^{2+} channel α_1-subunit riboprobes CaCh1–4. Each lane contains 5 μg of total (brain, heart, and skeletal muscle) or poly(A)$^+$ (cortex, outer medulla, or inner medulla of kidney) RNA. The positions of size markers (BRL) of the indicated lengths in kb are shown.

Nephron Segment Localization. As a first step towards assigning functional roles to the various molecular species we have identified, their distribution along different segments of the nephron was studied by microdissected-tubule PCR. Fig. 5 shows a typical blot of PCR-amplified tubule samples, hybridized to the CaCh4 riboprobe. The aggregate results of 12 independent tubule dissections, summarized in Table 1, indicate that a PCR product that hybridized to CaCh4 could be detected in more than half of all DCT samples. The identity of this molecular species was confirmed by restriction analysis with frequently cutting enzymes, which yielded a digestion pattern identical to that of the CaCh4 clone, RKC1.

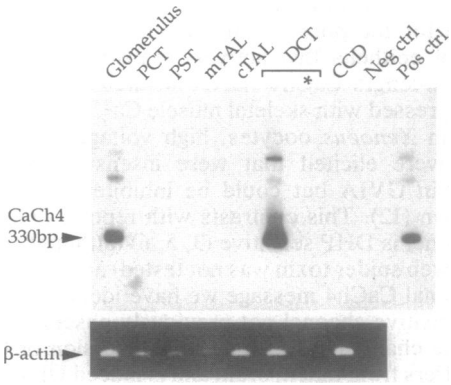

FIG. 5. Localization of expression of CaCh4 by microdissected-tubule PCR. (*Upper*) Typical blot of Cc1/2-amplified products hybridized to the CaCh4 probe. (*Lower*) β-actin expression in the same samples is demonstrated by ethidium bromide staining of Ac1/2 amplification products separated on a polyacrylamide gel. PCT, proximal convoluted tubule; PST, medullary proximal straight tubule; mTAL, medullary thick ascending limb; cTAL, cortical thick ascending limb; CCD, cortical collecting duct; *, no-reverse-transcriptase negative control; Neg ctrl, no-tubule negative control; Pos ctrl, amplified products from whole kidney cortex.

Table 1. Distribution of Ca^{2+} channel α_1-subunit expression by microdissected-tubule PCR

Sample	No. of samples*	No. positive†	
		CaCh1	CaCh4
Glomerulus	5 (3)	0	2
PCT	8 (4)	0	1
PST	2 (1)	0	0
mTAL	8 (6)	1	0
cTAL	6 (4)	0	0
DCT	8 (4)	0	5
CCD	4 (4)	0	1
Neg ctrl	9 (9)	0	0

PCT, proximal convoluted tubule; PST, medullary proximal straight tubule; mTAL, medullary thick ascending limb; cTAL, cortical thick ascending limb; CCD, cortical collecting duct; Neg ctrl, negative control without tubules.

*Includes only samples with detectable β-actin message. The number of animals is shown in parentheses.

†Number of tubule samples in which a PCR product of the expected size was detectable by blot hybridization to a probe specific for the indicated isoform. Cc1/2-amplified products were used for detection of CaCh1, 2, and 4, while Cc3/4 products were used for CaCh3. No signal was observed for either CaCh2 or CaCh3 in any of the samples.

Three DCT samples which were positive for β-actin had no detectable CaCh4, suggesting that CaCh4 might be expressed only in a subpopulation of all DCT segments. Alternatively, the RNA in those samples may have been partially degraded, in which case less abundant messages, such as CaCh4, would be likely to be lost before more abundant ones, such as β-actin. CaCh4 could also be detected in some samples of glomeruli, proximal convoluted tubule, and cortical collecting duct, suggesting that it is expressed at very low levels, close to the threshold for detection by our techniques.

Apart from medullary thick ascending limb and proximal straight tubule, we have exclusively confined our analysis to cortical nephron segments. Thus, the absence of CaCh1, -2, and -3 message in the nephron segments we analyzed may indicate that these molecular species originate from nontubule cells such as those of the interstitium, blood vessel wall, or intrarenal nerve endings, or alternatively that they are primarily expressed in medullary segments of the nephron (as seems likely from our Northern analysis of the renal expression of CaCh1 and -2).

Our finding of CaCh4 expression in the DCT, consistent with its cortical localization by Northern analysis, makes it a candidate for the pore-forming subunit of the apical Ca^{2+} channel of epithelia that actively reabsorb Ca^{2+}. Of note, when a full-length CaCh4 cDNA isolated from rabbit brain was coexpressed with skeletal muscle Ca^{2+} channel α_2 and β subunits in *Xenopus* oocytes, high voltage-activated Ca^{2+} currents were elicited that were insensitive to DHP or ω-conotoxin GVIA but could be inhibited by funnel web spider toxin (12). This contrasts with reports that the renal Ca^{2+} channel is DHP sensitive (3, 5, 6) (although sensitivity to funnel web spider toxin was not tested) and suggests either that the renal CaCh4 message we have identified encodes a DHP-insensitive channel not previously observed in kidney or that the channel constituted by expression of CaCh4 in kidney differs from that in brain and is indeed DHP sensitive. This could result from alternative splicing of CaCh4 itself, giving rise to a different α_1 subunit, or from association of the CaCh4 α_1 subunit with different accessory subunits, both of which could potentially alter the pharmacological characteristics of the channel (25).

Although the DCT is the principal site of active Ca^{2+} transport (1), the cortical thick ascending limb can also play a role, particularly when stimulated by parathyroid hormone (2). Thus, it is intriguing that no CaCh4 could be detected in the cortical thick ascending limb. This suggests either that CaCh4 is present at very low levels in this segment (consistent with the relatively minor active component of Ca^{2+} reabsorption) or that another channel type is expressed. It will therefore be interesting to determine the nephron segments in which the protein encoded by CaCh4 is expressed and to characterize the other subunits which form this channel.

Note Added in Proof. We have determined that the Cc3/4 primer pair used to detect CaCh3 expression is not sufficiently sensitive for microdissected tubule samples. Therefore, we are no longer confident that CaCh3 is absent from cortical nephron segments. This does not affect our tubule PCR analysis for CaCh1, 2, and 4 or our conclusions regarding the expression of CaCh4 in DCT.

We are grateful to Kwan-Dun Wu (Brigham and Women's Hospital) for providing several of the RNA samples used for Northern blots. This work was supported by a grant in aid (to J.L.) from the American Heart Association, by Research Grants DK42879 (to J.L.) and DK35930 (to B.M.B.) from the National Institutes of Health, and by a postdoctoral research fellowship from the National Kidney Foundation (to A.S.L.Y.).

1. Costanzo, L. S. & Windhager, E. E. (1978) *Am. J. Physiol.* **235**, F492–F506.
2. Friedman, P. A. (1988) *Am. J. Physiol.* **254**, F62–F70.
3. Bacskai, B. J. & Friedman, P. A. (1990) *Nature (London)* **347**, 388–391.
4. Merot, J., Poncet, V., Bidet, M., Tauc, M. & Poujeol, P. (1991) *Biochim. Biophys. Acta* **1070**, 387–400.
5. Matsunaga, H., Friedman, P. A., Kizer, N. & Stanton, B. A. (1991) *J. Am. Soc. Nephrol.* **2**, 627 (abstr.).
6. Lau, K., Quamme, G. & Tan, S. (1991) *J. Am. Soc. Nephrol.* **2**, 775 (abstr.).
7. Saunders, J. C. J. & Issacson, L. C. (1990) in *Calcium Transport and Intracellular Calcium Homeostasis*, eds. Pansu, D. & Bronner, F. (Springer, Berlin), pp. 27–34.
8. Hess, P. (1990) *Annu. Rev. Neurosci.* **13**, 337–356.
9. Tanabe, T., Takeshima, H., Mikami, A., Flockerzi, V., Takahashi, H., Kangawa, K., Kojima, M., Matsuo, H., Hirose, T. & Numa, S. (1987) *Nature (London)* **328**, 313–318.
10. Mikami, A., Imoto, K., Tanabe, T., Niidome, T., Mori, Y., Takeshima, H., Narumiya, S. & Numa, S. (1989) *Nature (London)* **340**, 230–233.
11. Hui, A., Ellinor, P. T., Krizanova, O., Wang, J.-J., Diebold, R. J. & Schwartz, A. (1991) *Neuron* **7**, 35–44.
12. Mori, Y., Friedrich, T., Kim, M.-S., Mikami, A., Nakai, J., Ruth, P., Bosse, E., Hofmann, F., Flockerzi, V., Furuichi, T., Mikoshiba, K., Imoto, K., Tanabe, T. & Numa, S. (1991) *Nature (London)* **350**, 398–402.
13. Dubel, S. J., Starr, T. V. B., Hell, J., Ahlijanian, M. K., Enyeart, J. J., Caterall, W. A. & Snutch, T. P. (1992) *Proc. Natl. Acad. Sci. USA* **89**, 5058–5062.
14. Perez-Reyes, E., Wei, X., Castellano, A. & Birnbaumer, L. (1990) *J. Biol. Chem.* **265**, 20430–20436.
15. Perez-Reyes, E., Kim, H. S., Lacerda, A. E., Horne, W., Wei, X., Rampe, D., Campbell, K. P., Brown, A. M. & Birnbaumer, L. (1989) *Nature (London)* **340**, 233–236.
16. Williams, M. E., Feldman, D. H., NcCue, A. F., Brenner, R., Velicelebi, G., Ellis, S. B. & Harpold, M. M. (1992) *Neuron* **8**, 71–84.
17. Llinàs, R., Sugimori, M., Lin, J.-W. & Cherksey, B. (1989) *Proc. Natl. Acad. Sci. USA* **86**, 1689–1693.
18. Sambrook, J., Fritsch, E. F. & Maniatis, T. (1989) *Molecular Cloning: A Laboratory Manual* (Cold Spring Harbor Lab., Cold Spring Harbor, NY).
19. Diebold, R. J., Koch, W. J., Ellinor, P. T., Wang, J.-J., Muthuchamy, M., Wieczorek, D. F. & Schwartz, A. (1992) *Proc. Natl. Acad. Sci. USA* **89**, 1497–1501.
20. Snutch, T. P., Tomlinson, W. J., Leonard, J. P. & Gilbert, M. M. (1991) *Neuron* **7**, 45–57.
21. Starr, T. V. B., Prystay, W. & Snutch, T. P. (1991) *Proc. Natl. Acad. Sci. USA* **88**, 5621–5625.
22. Nudel, U., Zakut, R., Shani, M., Neuman, S., Levy, Z. & Yaffe, D. (1983) *Nucleic Acids Res.* **11**, 1759–1771.
23. Moriyama, T., Murphy, H. R., Martin, B. M. & Garcia-Perez, A. (1990) *Am. J. Physiol.* **258**, F1470–F1474.
24. Malouf, N. N., McMahon, D. K., Hainsworth, C. N. & Kay, B. K. (1992) *Neuron* **8**, 899–906.
25. Varadi, G., Lory, P., Schultz, D., Varadi, M. & Schwartz, A. (1991) *Nature (London)* **352**, 159–162.